

Selective Post-Compensation of Nonlinear Impairments in Polarization-Division Multiplexed WDM Systems with Different Channel Granularities

Eduardo F. Mateo, Xiang Zhou, *Senior Member, IEEE*, and Guifang Li, *Senior Member, IEEE*

Abstract—Selective post-compensation of nonlinear impairments is investigated for polarization-division multiplexed-wavelength-division multiplexed (WDM) systems. A coupled system of nonlinear partial differential equations derived from the Manakov equations is used for digital backward propagation (DBP). Three WDM systems with different channel granularities have been simulated to evaluate the performance and computational load of vector DBP when different intra- and/or interchannel effects are compensated.

Index Terms—Chromatic dispersion compensation, digital signal processing, optical communications, optical Kerr effect, orthogonal frequency division multiplexing, quadrature amplitude modulation.

I. INTRODUCTION

RESEARCH in optical communications is being constantly driven by requirements for higher data rates and spectral efficiency. On one hand, higher bit rates per channel involve the deployment of high-order modulation formats, which require increased signal-to-noise ratio and, hence, higher power per channel. On the other hand, higher spectral efficiency also demands closely spaced channels to optimize the operational bandwidth of optical amplifiers. The above requirements clearly point to a scenario of increased nonlinearity in the form of intra- and interchannel effects. Therefore, the mitigation or compensation of fiber impairments which involve Kerr nonlinearity becomes crucial in future communications systems. In this vein, techniques capable of compensating the joint effect of chromatic dispersion and nonlinearity are gathering significant attention. In particular, digital backward propagation (DBP), which relies on reversing the optical transmission in the digital domain, is being considered as one of the candidates to be used in the future. DBP has been demonstrated numerically [1], [2] and experimentally [3] for coherent single-carrier wavelength-division multiplexed (WDM) systems. Recently, DBP has been also experimentally

demonstrated in a WDM system with polarization-division multiplexing (PDM) by solving, in the digital domain, the backward Manakov system [4]. To perform DBP using Manakov equations, the WDM channels are added coherently, upsampled, and backward-propagated as a whole [1]. Manakov equations include the compensation of interchannel four-wave mixing (FWM). Since FWM is sensitive to the relative phase of the channels, a set of phase-locked local oscillators (LOs) is required to preserve the relative phase of the WDM channels. To alleviate the cumbersome hardware and computational requirements for the compensation of FWM, a set of coupled nonlinear Schrödinger equations (NLSEs) can be implemented in the digital domain to compensate only self phase modulated (SPM) and cross-phase modulation (XPM) [5] for single-polarization WDM systems, which provides a noticeable improvement over dispersion compensation only. Furthermore, free-running LOs can be used and computation requirements are significantly relaxed [6]. In this paper, a coupled system of nonlinear partial differential equations is derived from the Manakov equations by neglecting the effects of FWM for PDM-WDM systems. This formulation enables the compensation of diverse interchannel and inter-polarization nonlinear effects on a channel-by-channel basis. These equations can isolate the contributions of SPM, XPM, and FWM allowing, therefore, selective compensation of nonlinearities. The efficacy and computational load of DBP are analyzed when different interchannel and cross-polarization effects are considered for PDM-WDM transmission. One of the advantages of using this set of coupled equations is that selective post-compensation of different intra- and/or interchannel nonlinear effects can be performed. This selective post-compensation has been applied to evaluate the performance and computational load of DBP in the context of PDM-WDM transmission and add/drop multiplexing, where information of adjacent channels may not be available at the receiver. In short, this paper focuses on the derivation of a new set of coupled equations for the implementation of DBP in PDM systems. Such equations allow the selective compensation of different nonlinear effects. This selective compensation can be used to analyze the performance of DBP in WDM systems with different granularities.

This paper is organized as follows. In Section II, the equations for DBP are derived and solved using a perturbative split-step method. In Section III, three PDM-WDM systems with a spectral efficiency of 4 bits/s/Hz are simulated where

Manuscript received May 21, 2010; revised August 4, 2010 and August 18, 2010; accepted September 5, 2010. Date of current version December 30, 2010.

E. F. Mateo and G. Li are with the Center for Research and Education in Optics and Lasers, College of Optics and Photonics, University of Central Florida, Orlando, FL 32816 USA (e-mail: emateo@creol.ucf.edu; li@creol.ucf.edu).

X. Zhou is with the AT&T Laboratory Research, Middletown, NJ 07748 USA (e-mail:zhoux@research.att.com).

Color versions of one or more of the figures in this paper are available online at <http://ieeexplore.ieee.org>.

Digital Object Identifier 10.1109/JQE.2010.2076792

different channel granularities are considered with a goal of assessing the effectiveness of channel-by-channel DBP. Concluding remarks are given in Section IV.

II. SELECTIVE POST-COMPENSATION OF NONLINEAR IMPAIRMENTS VIA VECTOR BACKWARD PROPAGATION

In a PDM-WDM system with coherent detection, the full reconstruction of the vector optical field can be achieved by using a polarization- and phase-diverse receiver. The reconstructed field will be used as the input for backward propagation in order to compensate the transmission impairments. Let E_{xm} and E_{ym} be the envelopes of x and y polarization tributaries of the received m th channel field where $m = 1, 2, \dots, N$ and N is the number of WDM channels. The reconstructed total optical field is given by $\mathbf{E} = \mathbf{x}E_x + \mathbf{y}E_y$, where $E_{(x,y)} = \sum_m \hat{E}_{(x,y)m} \exp(im\Delta\omega t)$ and $\Delta f = \Delta\omega/2$ is the channel spacing.

In general, optical communication fibers exhibit residual birefringence responsible for the random scattering of the state of polarization over a length scale of 10–100 m [7]. Moreover, the typical power values used in communication systems lead to rather long nonlinear lengths. Along the nonlinear length, the state of polarization changes fast and randomly, and the effect of the local state of polarization on the overall nonlinear interaction can be averaged over the entire Poincaré sphere. As a consequence of the above, the vector optical propagation can be described by the so-called Manakov system [4], [7], [8], which is expressed as follows for backward propagation:

$$-\frac{\partial E_{(x,y)}}{\partial z} + \frac{\alpha}{2} E_{(x,y)} + \frac{i\beta_2}{2} \frac{\partial^2 E_{(x,y)}}{\partial t^2} - \frac{\beta_3}{6} \frac{\partial^3 E_{x,y}}{\partial t^3} - i\frac{8}{9}\gamma (|E_{(x,y)}|^2 + |E_{(y,x)}|^2) E_{(x,y)} = 0 \quad (1)$$

where β_j represents the j th order dispersion, α is the absorption coefficient, γ is the nonlinear parameter, and t is the retarded time frame. The above system includes the effects of both coherent (FWM) and incoherent (SPM, XPM) nonlinear effects between channels and polarization components. The implementation of DBP can be realized using the split-step Fourier method (SSFM) [1], [7], where the linear and nonlinear terms in (1) can be uncoupled and solved sequentially over short distance segments (step size). As explained in [6], the coherent nature of FWM requires: 1) the full reconstruction of the entire WDM band; 2) enough upsampling to avoid aliasing of newly generated FWM products; 3) very short step sizes; and 4) phase-locked LOs to preserve the relative phase between channels.

Alternatively, interchannel coherent terms can be omitted in backward propagation by introducing the field expressions $E_{(x,y)}$ into (1), expanding the $|E_{(x,y)}|^2$ terms and ignoring phase-mismatched terms, leading to the following coupled equations:

$$-\frac{\partial \hat{E}_{(x,y)m}}{\partial z} + (L_m + S_m + C_{(x,y)m}) \hat{E}_{(x,y)m} + K_{(x,y)m} \hat{E}_{(y,x)m} = 0 \quad (2)$$

where L_m , S_m , $C_{(x,y)m}$, and $K_{(x,y)m}$ represent the linear dispersive operator, the SPM contribution, the XPM contribution, and a polarization mixing (PolM) term, respectively, given by

$$L_m = \frac{\alpha}{2} + D_{1m} \frac{\partial}{\partial t} + D_{2m} \frac{\partial^2}{\partial t^2} + D_{3m} \frac{\partial^3}{\partial t^3} \quad (3a)$$

$$S_m = -i\frac{8}{9}\gamma (|\hat{E}_{xm}|^2 + |\hat{E}_{ym}|^2) \quad (3b)$$

$$C_{(x,y)m} = -i\frac{8}{9}\gamma \left(\sum_{\forall q \neq m} 2|\hat{E}_{(x,y)q}|^2 + |\hat{E}_{(y,x)q}|^2 \right) \quad (3c)$$

$$K_{(x,y)m} = -i\frac{8}{9}\gamma \left(\sum_{\forall q \neq m} \hat{E}_{(y,x)q}^* \hat{E}_{(x,y)q} \right) \quad (3d)$$

with $D_{1m} = m\beta_2\Delta\omega - m^2\beta_3\Delta\omega^2/2$, $D_{2m} = i\beta_2/2 - m\beta_3\Delta\omega/2$ and $D_{3m} = -\beta_3/6$. Equation (2) neglects any interaction where the relative phase between the WDM channels is relevant. Moreover, when the PolM term $K_{(x,y)m}$ is included, the relative phase between the polarization components of each channel has to be preserved. This condition is typically fulfilled in polarization-diverse receivers, where each LO is split into orthogonal components to receive the PDM tributaries of each channel.

Equation (2) can also be solved using the SSFM. Here, the linear and nonlinear contributions can be uncoupled in a short segment of propagation (h). The linear part in (2) (i.e., $S_m = C_{(x,y)m} = K_{(x,y)m} = 0$) is solved in the frequency domain by using the following transfer function:

$$H_m(\omega) = \exp \left[\left(\frac{\alpha}{2} + i\beta_2 \frac{(\omega - m\Delta\omega)^2}{2} \right) h \right] \times \exp \left(i\beta_3 \frac{(\omega - m\Delta\omega)^3}{6} h \right). \quad (4)$$

The linear step has the following solution where \mathcal{F} represents the Fourier transform:

$$\hat{E}_{(x,y)m}(t, z+h) = \mathcal{F}^{-1} \{ \mathcal{F} [\hat{E}_{(x,y)m}(t, z)] H_m(\omega) \}. \quad (5)$$

Subsequently, the nonlinear part ($L_m = 0$) is solved. Here, two cases are considered: the case where only incoherent terms are considered ($K_{(x,y)m} = 0$), and the case where all nonlinear terms are considered. In the first case, the equation for the nonlinear step has the following exact solution:

$$\hat{E}_{(x,y)m}(z+h) = \hat{E}_{(x,y)m}(z) \exp[(S_m + C_{(x,y)m})h]. \quad (6)$$

In the second case, the nonlinear part of (2) lacks a closed-form solution since the intensities of the channels $|\hat{E}_{(y,x)q}|^2$ are no longer z -invariants. However, a perturbation approach can be performed using the solution given by (6) as the first-order solution

$$\hat{E}_{(x,y)m}^{(1)} = \hat{E}_{(x,y)m}^{(0)} + K_{(x,y)m}^{(0)} \hat{E}_{(x,y)m}^{(0)} h \quad (7)$$

where $\hat{E}_{(x,y)m}^{(0)}$ is the solution given by (6) and $K_{(x,y)m}^{(0)}$ is obtained from (3d) with the values $\hat{E}_{(x,y)m}^{(0)}$ as inputs. Equation (7) represents an approximate solution which requires h to be sufficiently small. The above formulation has the advantage

of being simple and straightforward, which is fundamental for an eventual DSP implementation. However, more complex solutions than the one given by (7) to increase the accuracy of the SSFM are possible.

Equation (2) can be used to compensate for different linear and nonlinear distortions at the receiver. Four cases are studied: chromatic dispersion compensation ($S_m = C_{(x,y)m} = K_{(x,y)m} = 0$); SPM compensation ($C_{(x,y)m} = K_{(x,y)m} = 0$); SPM + XPM compensation ($K_{(x,y)m} = 0$); and SPM + XPM + PolM compensation, where all the terms are included. For simplicity, we will refer to these cases as DBP1, DBP2, DBP3, and DBP4, respectively. In addition, we will refer as DBP5 the full compensation of nonlinear impairments, including FWM, using the Manakov system given by (1) [1], [6].

III. SIMULATION SETUP AND RESULTS

A. PDM-WDM Transmission System for Simulation: Transmitter/Receiver Configuration

With the goal of simulating the effectiveness of DBP for future high-capacity and high-spectral-efficiency optical transport systems, orthogonal frequency division multiplexing (OFDM) is chosen as the modulation format. At this point, it is important to note that DBP is independent of the modulation format and, therefore, its implementation is the same for either single-carrier or multicarrier modulation formats. The powerful electrical processing involved in the generation and detection of OFDM signals permits compact spectral shaping as well as scalability to higher order modulation formats. In addition, a multiband implementation of OFDM channels using frequency combs has recently enabled transmission in the Tb/s/channel range, overcoming the digital-to-analog converter (DAC)/analog-to-digital data converter (ADC) limitations inherent to OFDM [9], [10].

Fig. 1 illustrates the multiband coherent OFDM system with DBP post-compensation using coupled NLSEs. A set of phase-locked tones are generated, modulated, and added coherently to create the OFDM channel (see transmitter inset in Fig. 1). Assuming, for example, a DAC analog bandwidth of 5 GHz, a multiband OFDM signal of 100 Gbaud can be generated by using a frequency comb consisting of 20 lines separated by 5 GHz. Typically, phase-locked frequency lines are created from a laser source using a Mach-Zehnder modulator fed by a sinusoidal electrical signal [10]. Likewise, recirculating frequency shifters have been also used for the same purpose, achieving similar results without requiring high driving voltages [11], [12]. At the receiver side, each multiband channel is demultiplexed, detected, and postprocessed using DBP. Demultiplexing is performed by using ideal rectangular-shaped optical band-pass filters with a bandwidth twice the baud rate. The detection of each channel is eventually limited, in this case, by the bandwidth of the ADCs. Here, frequency combs are created at the receiver to act as a set of phase-locked LOs. Similar to the transmitter case, each channel is again separated into sub-bands, each of which is detected coherently on an individual basis (see inset in Fig. 1). After detection and digitization, the sub-bands are upsampled and coherently added to reconstruct the envelope of each channel,

$\hat{E}_{(x,y)m}$. Without loss of generality, Fig. 1 shows the same number of sub-bands at transmitter and receiver. However, bandwidth limitations are not necessarily equivalent at both sides. Hence, the number of sub-bands at the transmitter can be different since practical ADCs are capable of handling larger bandwidth than DACs. Once the envelopes $\hat{E}_{(x,y)m}$ are obtained, backward propagation is performed using (2). Next, the OFDM signal is demodulated via fast Fourier transform (FFT) and polarization demultiplexing is performed. For the sake of completeness, results for FWM compensation will be shown later. In this case, the configuration shown in Fig. 1 is no longer valid since the coherent reconstruction of the entire WDM band is necessary for each polarization component before DBP. Hence, all LOs used for the detection of each channel for each polarization have to be phase-locked. Details of the receiver configuration for FWM compensation can be found in [6].

Three PDM-WDM systems with the same spectral efficiency of 4 bits/s/Hz will be simulated: 3×800 , 6×400 , and 12×200 Gb/s with a channel spacing of 200, 100, and 50 GHz, respectively. The above systems operate at 100, 50, and 25 Gbaud, respectively, modulated in a 16 quadrature amplitude modulation (QAM)-OFDM format. For simplicity and according to the channel granularity, the above systems will be referred as coarse, medium, and fine grids. A total of 8192 symbols encoded in a 16 QAM format are modulated into 128 OFDM subcarriers with symbol lengths of 1.28, 2.56, and 5.12 ns, respectively. Therefore, a total of 64 independent OFDM symbols are simulated. Since DBP inherently performs dispersion compensation, no cyclic prefix overhead is necessary. Time-interleaved training symbols are used for polarization demultiplexing [13]. For each WDM system, simulations are performed for input power values spanning from 3 to 21 dBm (total optical power including WDM channels and polarization tributaries). The fiber length is $L = 10 \times 100$ km with a dispersion parameter of $D = 16$ ps/km/nm and a dispersion slope of $D_s = 0.08$ ps/km/nm. The loss is $\alpha = 0.2$ dB/km, nonlinearity is $\gamma = 1.31$ W⁻¹km⁻¹, and EDFAs have a noise figure of 5 dB. The WDM band is centered at 1550 nm. Forward transmission has been simulated by using virtual photonics instrument (VPI) TransmissionMaker, whereas backward propagation is performed independently in MATLAB. Forward transmission is simulated by modeling random birefringence and solving the exact nonlinear propagation equations [7, Eqs. 6.1.11–12]. The rate of variation of the random birefringence is modeled using VPI by using a Gaussian distribution with a variance inversely proportional to the fiber correlation length, which is assumed to be 50 m. For simplicity, our simulations neglect laser phase noise and polarization mode dispersion (i.e., the differential group delay is zero). Unlimited bandwidth for detectors, modulators, and DACs/ADCs is assumed. For the Q -factor calculation, each constellation cluster is isolated and the standard deviations of the real and imaginary parts are obtained. The Q -factor is obtained by dividing the standard deviations by the mean values of the real and imaginary parts of each cluster. Finally, the values are averaged over the 16 clusters. The sampling rate requirements for FWM

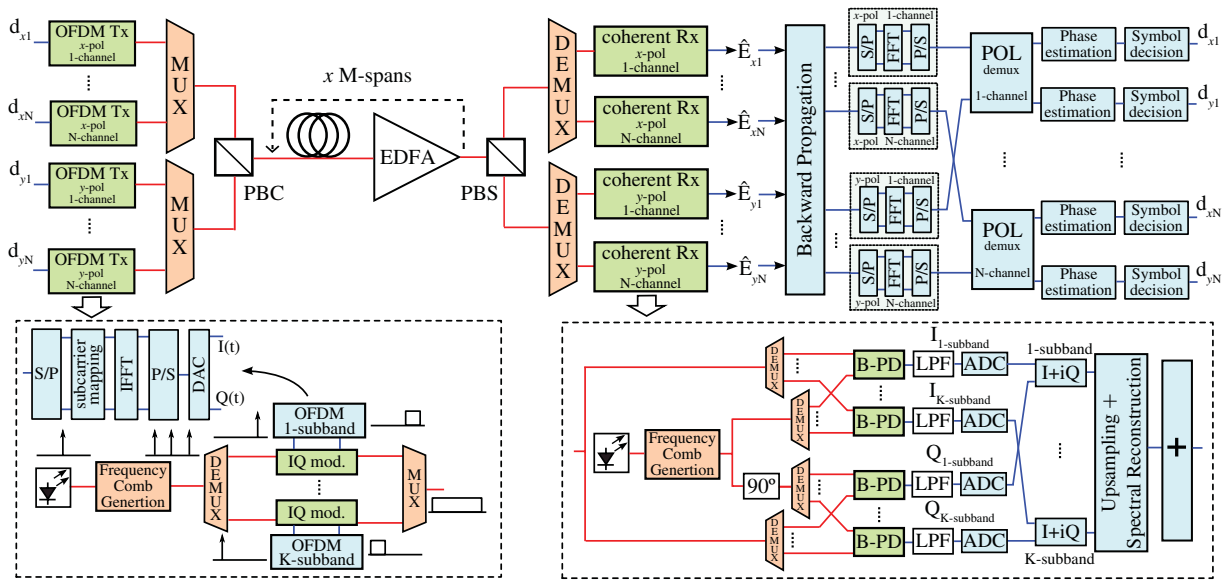


Fig. 1. Scheme of the WDM transmission system using multiband PDM-OFDM channels. PBC/PBS: Polarization beam combiner/splitter, B-PD: Balanced photo-detectors, LPF: Low-pass filter.

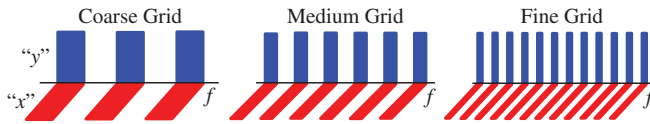


Fig. 2. Simulated WDM systems with coarse, medium, and fine granularity.

and XPM compensation have been reported in [6]. In this simulation, forward propagation has been performed with a sampling rate of 1600 Gsamples/s. For backward propagation, the channels are downsampled to 2 samples/symbol for all the DBP schemes with the exception of DBP5, where no downsampling is performed to avoid the aliasing of newly generated FWM products [6].

B. Simulation Results: Noninterleaved Polarization-Division Multiplexing

For the case of noninterleaved PDM-WDM transmission system considered here, each WDM channel carries two polarization tributaries at the same wavelength as shown in Fig. 2.

Simulation results are shown in Fig. 3. The performance (Q -factor) of the different DBP schemes is plotted as a function of the channel launching power.

Regardless of the degree of granularity, the simulation results show a significant improvement in the performance when XPM and PolM terms are included in the backward propagation equations. Particularly, it is interesting to note the importance of the PolM term (included in DBP4), which is present only in PDM transmission. Including the PolM term yields results that are almost identical to the total impairment compensation case (DBP5), which is only limited by amplified spontaneous emission (ASE) and ASE-seeded nonlinearities. Therefore, for standard single-mode fibers and channel spacing higher than 50 GHz, FWM effects can be neglected in the DBP

equations with a negligible penalty. It is important to recall that DBP4 requires only knowledge of the relative phase between the two polarization tributaries within each WDM channel. Consequently, the LOs used in each coherent Rx in Fig. 1 are not required to be phase-locked.

By comparing the three different granularities, the most significant difference appears in the DBP2 case, where only intrachannel nonlinearities are compensated. Here, the larger channel spacing of the coarse grid yields a much stronger mitigation of interchannel effects, resulting in a 2-dB improvement in the Q -factor with respect to DBP1. On the contrary, the fine grid is exposed to stronger interchannel effects, which modify the received waveforms enough to make DBP2 inefficient and almost equivalent to dispersion compensation only. The results obtained for DBP2 reveal the sensitivity of DBP to the initial conditions, where relatively weak interchannel effects have a clear impact on the DBP propagation performance. To assess the impact of interchannel nonlinearities in DBP, a single-channel transmission system (1×800 Gb/s) has been simulated. Fig. 4 shows the performance of single-channel transmission compared to the 3×800 Gb/s WDM case. Fig. 4 reveals no significant difference in the Q -factor between the single-channel and the WDM cases for DBP1. However, when intrachannel nonlinear effects are compensated (DBP2), the difference in performance between single channel and WDM becomes remarkable. The small difference observed for DBP1 is mainly attributed to the dominance of SPM with respect to XPM. However, that small difference in the Q -factor does not necessarily reflect the real difference of the waveforms. Such difference is important for DBP due to its sensitivity to the initial conditions. Such sensitivity explains the poor performance of DBP2 for the WDM case.

Together with the performance of DBP in terms of nonlinearity mitigation, the computation requirements of DBP are important when performance versus cost is considered.

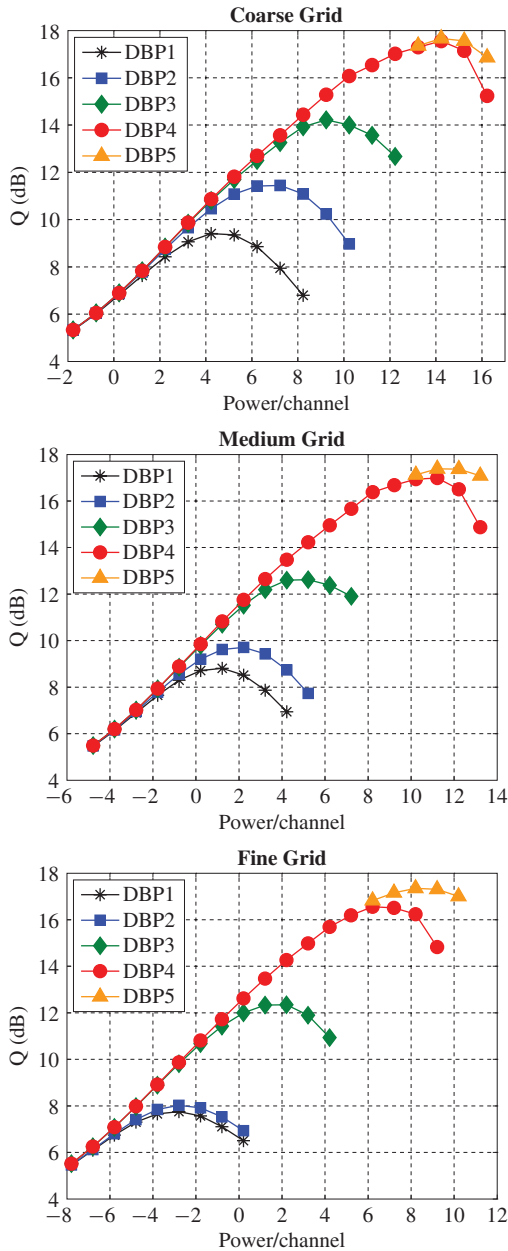


Fig. 3. Q -factors versus channel powers for each WDM system and DBP scheme. Q -factors are the result of averaging over WDM channels and polarization tributaries. DBP1 represents dispersion compensation, DBP2 includes SPM compensation, DBP3 includes XPM compensation, and DBP4 includes PolM. Finally, DBP5 represents full impairment compensation including FWM.

A rigorous calculation of the number of operations required for DBP involves the analysis of the overlap-add method [14]. Such method is used for the frequency-domain implementation of the dispersion operator in the SSM, given by (4). This requires the optimization of the sample block-length as a function of the SSFM step size. Although the total number of operations is important, this paper focuses on the performance and relative computational requirements of each compensation scheme. For this comparison purpose, the number of steps for the SSFM is used. The optimum number of steps corresponds to a Q -value penalty of approximately 0.1 dB with respect to the plateau value.

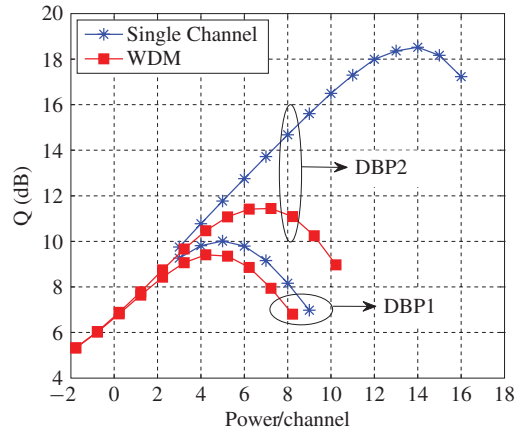


Fig. 4. Q -factor versus channel powers comparing single-channel and WDM transmission for the 800-Gb/s case.

Fig. 5 shows the number of steps (computation requirements) of the SSFM for each DBP and WDM granularity. In addition, Table I summarizes the results including the optimum number of steps shown in Fig. 5. For intrachannel compensation (DBP2), it is shown that the required step size is proportional to the dispersion length of each channel. This makes the number of steps to be proportional to the square of the channel bandwidth, $n_{steps}^{DBP2} \propto B^2$, which agrees with the numbers in Table I, where the number of steps approximately increases by a factor of four as the channel bandwidth doubles. With respect to the compensation of XPM (DBP3), it was found in [5] that the optimum step size for XPM compensation was correlated with the minimum walk-off length between channels. By following the formalism in [5], the optimum step size in a walk-off limited system is given by

$$h^{XPM} = \frac{3}{2} \frac{1}{4\pi[(N-1)\Delta f + B]B} \quad (8)$$

where B is the channel bandwidth. According to the above expression, the optimum number of steps is 429, 235, and 123 for the coarse, medium, and fine grids, respectively. The above numbers agree fairly well with the numbers shown in Table I for the DBP3 case. When PolM terms are included (DBP4), an increase in the number of steps is observed. In this case, it must be noted that the optimum power is increased by 5 dB from DBP3 to DBP4. Likewise, new terms contribute to the nonlinear phase shift. Therefore, a reduced step size is necessary due to an increased nonlinearity. Finally, the compensation of FWM (DBP5) requires a significantly larger number of steps, as shown in [5]. Here, the number of steps scales with the total WDM bandwidth and, therefore, no difference is observed with the granularity.

C. Simulation Results: Interleaved Polarization Multiplexing

The results in Section III-B demonstrate that inclusion of the PolM terms in DBP enhance the performance to a point comparable to the full compensation of impairments including FWM. However, this performance improvement is achieved at the expense of additional computational effort due to the increased optimum power. The role of the PolM terms should be different if interleaved PDM is employed, where the

TABLE I

SUMMARY OF PERFORMANCE (OPTIMUM Q -FACTOR, OPTIMUM NUMBER OF STEPS PER SPAN, AND OPTIMUM POWER) FOR THE NONINTERLEAVED WDM SYSTEMS, WHERE DBP1 REPRESENTS DISPERSION COMPENSATION, DBP2 INCLUDES SPM COMPENSATION, DBP3 INCLUDES XPM COMPENSATION, AND DBP4 INCLUDES POLM. FINALLY, DBP5 REPRESENTS FULL IMPAIRMENT COMPENSATION INCLUDING FWM

	Coarse grid			Medium grid			Fine grid		
	Q (dB)	Steps/span	P (dBm)	Q (dB)	Steps/span	P (dBm)	Q (dB)	Steps/span	P (dBm)
DBP1	9.3	1	5.2	8.8	1	1.2	7.7	1	-2.8
DBP2	11.4	40	7.2	9.7	10	2.2	8.0	2	-2.8
DBP3	14.2	400	9.2	12.6	200	5.2	12.3	100	7.2
DBP4	17.5	600	14.2	16.9	350	11.2	16.5	200	7.2
DBP5	17.6	4000	14.2	17.4	4000	11.2	17.3	4000	8.2

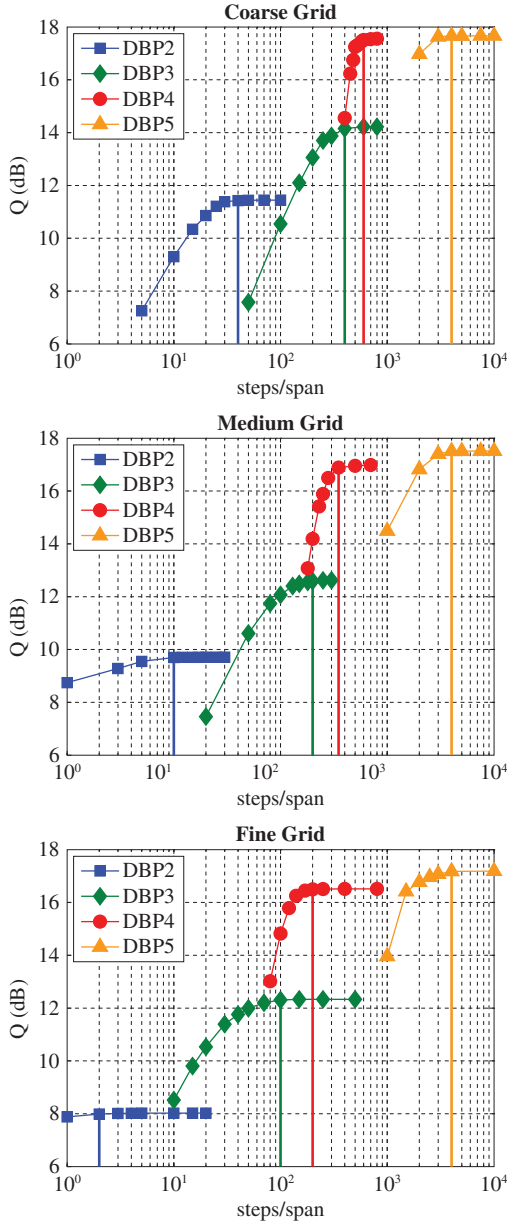


Fig. 5. Q -factor versus step number for each WDM system and DBP scheme. Solid vertical lines indicate the optimum step number per span.

polarization tributaries are shifted by a frequency of $\delta = \Delta f/2$ as shown in Fig. 6.

For the interleaved PDM-WDM case, total optical field is given by $\mathbf{E} = \mathbf{x}E_x + \mathbf{y}E_y$, where now $E_x =$

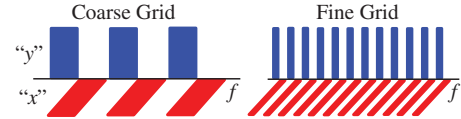


Fig. 6. WDM systems using PDM-OFDM channels with interleaved polarization multiplexing.

$\sum_m \hat{E}_{xm} \exp(im\Delta\omega t)$ and $E_y = \sum_m \hat{E}_{ym} \exp(im\Delta\omega t - i2\pi\delta t)$. By introducing the above expressions for the envelopes into (1), it is easy to demonstrate that the terms $K_{(x,y)m}$ are no longer phase-matched since the polarization tributaries experience dispersive walkoff due to the frequency shift δ . Such phase mismatch mitigates any FWM contribution, including the PolM terms, and the compensation of SPM + XPM (DBP3) is expected to improve with respect to the noninterleaved case. Backward propagation for polarization interleaving (Fig. 6) has been performed using a slightly different version of (2). Now, the linear operator L_m is split into L_{mx} and L_{my} for each polarization component, according to the frequency shift δ . Therefore, the linear operators, now in the frequency domain, become $H_{mx}(\omega) = H(\omega)$ and $H_{my}(\omega) = H(\omega - 2\pi\delta)$, where $H(\omega)$ is given by (4). The terms S_m and $C_{(x,y)m}$ remain formally identical, whereas the term $K_{(x,y)m}$, now including dispersive phase-mismatch, is neglected.

Fig. 7 shows the performance of backward propagation for polarization interleaving compared to the noninterleaved case. Results are shown for the coarse and fine grids. As expected, the results show the effectiveness of DBP3 when polarization interleaving is employed. Now, the dispersive phase mismatch between polarization tributaries mitigates coherent mixing effects, which makes incoherent effects more dominant. The required number of steps for DBP3 is shown in Fig. 8, comparing the interleaved and the noninterleaved configurations. The increased number of steps observed in Fig. 8 for the interleaved case can be explained as follows. For the coarse grid, the minimum walk-off length is reduced significantly in the interleaved case. In fact, one can demonstrate that the minimum walkoff between the edge polarization tributaries is now given by

$$h^{XPM} = \frac{3}{2} \frac{1}{4\pi[(N-1)\Delta f + 2B]B} \quad (9)$$

which gives a number of steps of 515 compared to the 429 obtained for the noninterleaved case. However, this number is still quite different from 600, which is the optimum value

TABLE II

SUMMARY OF PERFORMANCE (OPTIMUM Q -FACTOR, OPTIMUM STEP NUMBER/SPAN, AND OPTIMUM POWER) FOR THE INTERLEAVED WDM SYSTEMS SHOWN IN FIG. 6

	Coarse grid			Fine grid		
	Q (dB)	Steps	P (dBm)	Q (dB)	Steps	P (dBm)
DBP3	16.0	600	12.2	15.2	175	5.2

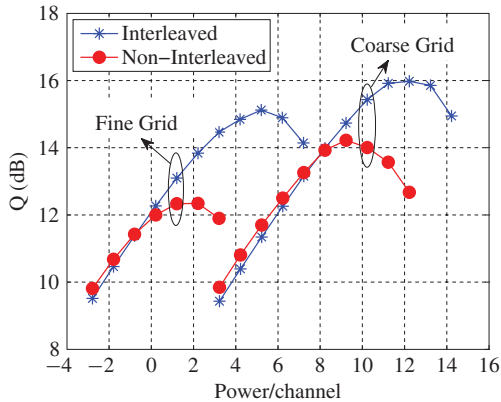


Fig. 7. Q -factor versus power comparison between the interleaved and noninterleaved cases. Results are shown for the compensation of SPM + XPM effects (DBP3).

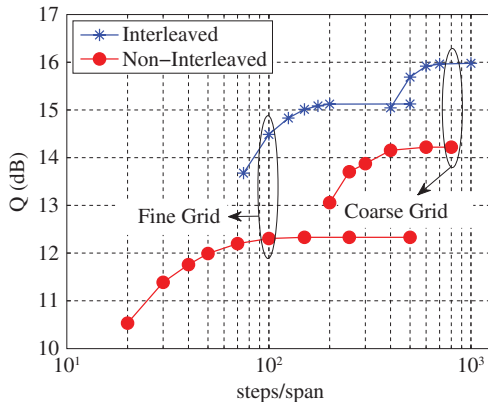


Fig. 8. Q -factor versus step-number comparison between the interleaved and noninterleaved cases. Results are shown for the compensation of SPM + XPM effects (DBP3).

shown in Fig. 7. To explain this discrepancy, one must look at the optimum power values. As shown in Fig. 7, a 3-dB increase in the optimum power is observed when polarization interleaving is employed. Therefore, the increased nonlinear phase shift forces the number of steps to grow. The results are summarized in Table II for the interleaved WDM configuration. From a practical point of view, interleaved polarization multiplexing allows a more efficient compensation of nonlinearities with no phase-locking requirements between polarization tributaries. Typical polarization-diverse receivers use a single LO and a polarization beam splitter to detect each polarization component. However, thermal or mechanical instabilities induce fluctuations in the optical paths and the phase relationship may not be preserved between polarization components. This phase mismatch impairs DBP4 and eventually has to be corrected before backward propagation. Interleaved

polarization multiplexing overcomes this limitation, allowing increased tolerance of the receiver components.

IV. CONCLUSION

The selective post-compensation of nonlinearities was studied for polarization-multiplexed WDM transmission. A coupled system of nonlinear partial differential equations was derived from the Manakov system for DBP. Such system enabled the selective compensation of intra- and interchannel effects as well as inter-polarization interactions.

Selective nonlinearity compensation using DBP was simulated for PDM-WDM systems with different channel granularities while maintaining the overall spectral efficiency. Our results show that, even for large channel spacing and large accumulated dispersion, interchannel nonlinear effects have to be included in the DBP for a substantial performance improvement. In particular, a new term has been included in the coupled equations to compensate for phase-matched PolM. This effect does not have a counterpart in the single-polarization transmission, i.e., scalar DBP, and plays an important role in both performance and computational cost.

From a practical point of view, our results show that the compensation of nonlinear intrachannel effects, i.e., channel-by-channel nonlinearity compensation, becomes completely inefficient when the channel spacing reaches a certain lower limit. In particular, in the 4-bit/s/Hz PDM-WDM system, intrachannel compensation improves the performance provided that channel spacing is larger than 100 GHz. As a consequence, network elements such add/drop multiplexers impose a limit on the applicability of DBP since the information of dropped neighboring channels is unavailable and only intrachannel effects can be corrected. However, channel-by-channel post-compensation using DBP could still be effective for coarse granularity with large bit rates and large channel spacing. On the other hand, for point-to-point links in which all WDM channels share the same Tx-Rx locations, DBP for post-compensation of interchannel nonlinearities is possible and effective.

REFERENCES

- [1] X. Li, X. Chen, G. Goldfarb, E. F. Mateo, I. Kim, F. Yaman, and G. Li, "Electronic post-compensation of WDM transmission impairments using coherent detection and digital signal processing," *Opt. Exp.*, vol. 16, no. 2, pp. 880–888, Jan. 2008.
- [2] E. Ip and J. M. Kahn, "Compensation of dispersion and nonlinear impairments using digital backpropagation," *J. Lightw. Technol.*, vol. 26, no. 20, pp. 3416–3425, Oct. 2008.
- [3] G. Goldfarb, M. G. Taylor, and G. Li, "Experimental demonstration of fiber impairment compensation using the split-step finite-impulse-response filtering method," *IEEE Photon. Technol. Lett.*, vol. 20, no. 22, pp. 1887–1889, Nov. 2008.
- [4] F. Yaman and G. Li, "Nonlinear impairment compensation for polarization-division multiplexed WDM transmission using digital backward propagation," *IEEE J. Photon.*, vol. 1, no. 2, pp. 144–152, Aug. 2009.
- [5] E. F. Mateo, L. Zhu, and G. Li, "Impact of XPM and FWM on the digital implementation of impairment compensation for WDM transmission using backward propagation," *Opt. Exp.*, vol. 16, no. 20, pp. 16124–16137, Sep. 2008.
- [6] E. F. Mateo and G. Li, "Compensation of interchannel nonlinearities using enhanced coupled equations for digital backward propagation," *Appl. Opt.*, vol. 48, no. 25, pp. F6–F10, Sep. 2009.
- [7] G. P. Agrawal, *Nonlinear Fiber Optics*, 4th Ed. New York: Academic, 2005.

- [8] D. Marcuse, C. R. Menyuk, and P. K. A. Wai, "Application of the Manakov-PMD equation to studies of signal propagation in optical fibers with randomly varying birefringence," *J. Lightw. Technol.*, vol. 15, no. 9, pp. 1735–1746, Sep. 1997.
- [9] W. Shieh, H. Bao, and Y. Tang, "Coherent optical OFDM: Theory and design," *Opt. Exp.*, vol. 16, no. 2, pp. 841–859, Jan. 2008.
- [10] R. Dirschler and F. Buchali, "Transmission of 1.2 Tb/s continuous waveband PDM-OFDM-FDM signal with spectral efficiency of 3.3 bit/s/Hz over 400 km of SSMF," in *Proc. Conf. OFC, OSA*, San Diego, CA, Mar. 2009, no. PDPC2, pp. 1–3.
- [11] Y. Ma, Q. Yang, Y. Tang, S. Chen, and W. Shieh, "1-Tb/s per channel coherent optical OFDM transmission with subwavelength bandwidth access," in *Proc. Conf. OFC, OSA*, San Diego, CA, Mar. 2009, no. PDPC1, pp. 1–3.
- [12] S. Chandrasekhar, X. Liu, B. Zhu, and D. W. Peckham, "Transmission of a 1.2-Tb/s 24-carrier no-guard-interval coherent OFDM superchannel over 7200-km of ultralarge-area fiber," in *Proc. 35th Eur. Conf. Opt. Commun.*, Sep. 2009, no. PD2.6, pp. 1–2.
- [13] S. L. Jansen, I. Morita, T. C. Schenk, and H. Tanaka, "Long-haul transmission of 16×52.5 Gbits/s polarization-division-multiplexed OFDM enabled by MIMO processing (Invited)," *J. Opt. Netw.*, vol. 7, no. 2, pp. 173–182, Feb. 2008.
- [14] P. Poggiolini, A. Carena, V. Curri, and F. Forghieri, "Evaluation of the computational effort for chromatic dispersion compensation in coherent optical PM-OFDM and PM-QAM systems," *Opt. Exp.*, vol. 17, no. 3, pp. 1385–1403, Feb. 2009.

Eduardo F. Mateo received the Ph.D. degree in physics from the University of Santiago de Compostela, Galicia, Spain, in 2005.

He is currently a Research Scientist at the Center for Research and Education in Optics and Lasers, College of Optics and Photonics, University of Central Florida, Orlando. His current research interests include coherent optical communications, all-optical devices, and nonlinear fiber optics.

Xiang Zhou (M'00–SM'05) received the Ph.D. degree in electrical engineering from Beijing University of Posts & Telecommunications, Beijing, China, in 1999.

He was with Nanyang Technological University, Singapore, as a Research Fellow, carrying out research on optical code division multiple access and wide-band Raman amplification from 1999 to 2001. Since October 2001, he has been a Senior Member of the Technical Staff in AT&T Laboratory Research, Middletown, NJ. He has authored more than 60 papers in prestigious journals/conference proceedings and holds 20 U.S. patents. His current research interests include various aspects of long-haul optical transmission and photonic networking technologies, including Raman amplification, polarization-related impairments, optical power transient control, advanced modulation formats, and digital signal processing at bit rates of 100 Gb/s and beyond.

Dr. Zhou is a member of the Optical Society of America. He currently serves as an Associate Editor of *Optics Express*.

Guifang Li (SM'99) received the Ph.D. degree in electrical engineering from the University of Wisconsin, Madison, in 1991.

He is currently a Professor of optics, electrical and computer engineering, and physics at the Florida Photonics Center of Excellence, University of Central Florida (UCF), Orlando. His current research interests include optical communications and networking, RF photonics, and all-optical signal processing.

Dr. Li is the recipient of the National Science Foundation CAREER Award, the Office of Naval Research Young Investigator Award, and the UCF Research Incentive Award. He is a Fellow of the Society of Photo-Optical Instrumentation Engineers, and the Optical Society of America. He currently serves as an Associate Editor for IEEE PHOTONICS TECHNOLOGY LETTERS and a Deputy Editor for *Optics Express*.